6-1969

A Nonsecond Time-of-Flight Spectometer

David Moorman
Western Kentucky University

Moorman,

David K.

1969

A NANOSECOND
TIME-OF-FLIGHT SPECTROMETER

BY

DAVID K. MOORMAN

A THESIS

SUBMITTED IN PARTIAL FULFILLMENT

OF THE REQUIREMENTS FOR THE DEGREE OF

MASTER OF SCIENCE IN ENGINEERING PHYSICS

WESTERN KENTUCKY UNIVERSITY

JUNE 1969

A NANOSECOND

TIME-OF-FLIGHT SPECTROMETER

APPROVED May 22, 1969
(Date)

A. L. Humphrey
Thesis Advisor

B. L. Hall

N. F. Lif

John D. Winston
Dean of the Graduate School

ACKNOWLEDGMENTS

The author wishes to extend his sincere appreciation to Dr. D. L. Humphrey for his many hours of discussion, direction, and work as thesis director, and to Mr. L. McGimsey for his time and assistance in taking the time-of-flight data. He would like to extend his sincere appreciation to the Faculty Research Fund of Western Kentucky University for their financial assistance on this project.

The author wishes to extend his sincere appreciation to the people associated with the Tube Department of the General Electric Company at Owensboro, Kentucky, for their help and cooperation on this project. Some members of the Tube Department he would mention especially: Mr. C. Hopper, Jr., Manager of Engineering, Microwave Devices Section, who made available the laboratory where most of the work was done to assemble the electronic circuits; Mr. C. L. Reynolds, Manager of Microwave Devices Unit, who supplied the equipment for the testing of the electronic circuits; Mrs. Violet Jackson, who performed the chemical etching necessary to fabricate the electronic circuits; and Mrs. Dorothy Henning, who faithfully typed the many copies of the manuscript.

The author's deepest appreciation is for his wife, Doris, who assisted in reading the manuscript and provided encouragement and criticism at just the right times.

TABLE OF CONTENTS

LIST OF TABLES

LIST OF ILLUSTRATIONS

I. INTRODUCTION

The neutron is a valuable experimental projectile for studying the nuclear force field. The neutron is a neutral particle, and hence it does not experience the coulomb field surrounding the nucleus. Nuclear interactions can then be studied at low bombarding energies. If significant information about the nuclear interaction is desired, the energy spectrum of the neutrons must be determined. Since the discovery of the neutron by Chadwick in 1932, many techniques have been devised to detect and accurately measure the energy of neutron beams. One of the older and better known methods of measuring the energy of neutrons is by proton recoil. This method of spectrometry is based on the principle that a neutron, incident upon a hydrogeneous target, will have an elastic collision with a proton in the target. The recoil protons are distributed isotropically through all angles in the forward hemisphere. The energy of the recoil proton is proportional to the $\cos^2\theta$ where θ is the angle of the recoil proton. The maximum energy acquired by the proton occurs in a head-on collision in which all the energy of the incident neutron is transferred to the proton. The energy spectrum of the recoil protons that occurs in an organic scintillator is shown in Fig. 1 (solid curve)[1]. The value E_n is the incident neutron energy. The experimental curve (Fig. 1, dashed curve) differs from the theoretical curve because of a non-linear response

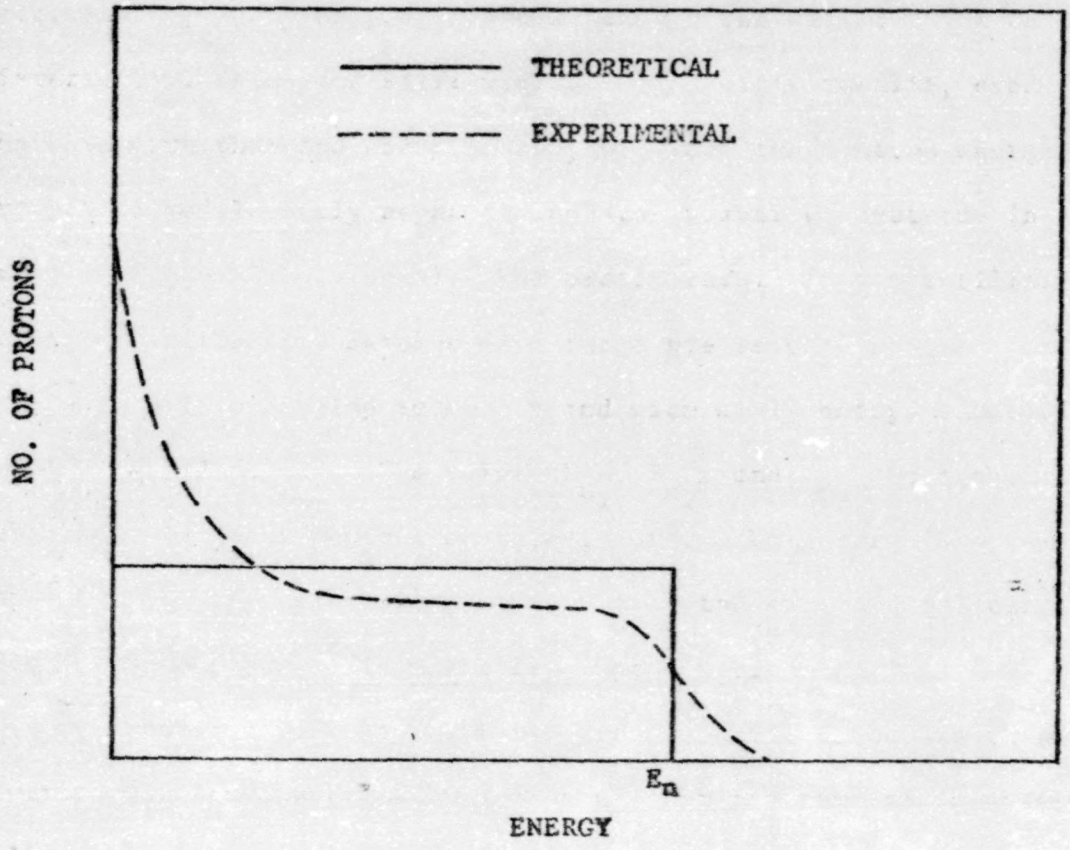

FIGURE 1 THE NUMBER OF RECOIL PROTONS AS A FUNCTION OF PROTON ENERGY.[1]

of the scintillator to the recoil proton, statistical fluctuations of light from the scintillator, and statistical fluctuations in the conversion that takes place in the photomultiplier.

If the neutrons are monoenergetic, an accurate experimental determination of E_n is possible even though the experimental curve is distorted. This method still yields satisfactory results, even if there is more than one energy group, provided the neutron energy groups are sufficiently separated and the number of neutrons in each group is approximately equal. The proton recoil in a scintillator yields unsatisfactory results when there are several neutron energy groups of widely varying intensity and with small energy separations (Fig. 2, solid curve). The values E_{n_1}, E_{n_2}, and E_{n_3} are the respective incident neutron energies. It can be observed that separation of the three energy groups from the experimental curve (Fig. 2, dashed curve) is virtually impossible.[2]

Another difficulty with the proton recoil method is that neutrons with an energy of 10 Mev or greater can have an inelastic collision with protons.

Proton recoil measurements are made in most cases with an organic scintillation detector. If the detector is made thick enough to have a very high detection efficiency for neutrons, the spectrum is distorted by multiple scattering of the neutrons in the scintillator. Also, a thick detector has a higher efficiency for gamma rays which produce unwanted interactions in the scintillator.

Another method of measuring the energy spectrum of neutrons is by a time-of-flight spectrometer. The energy of the neutron group is determined by measuring the time-of-flight over a known distance

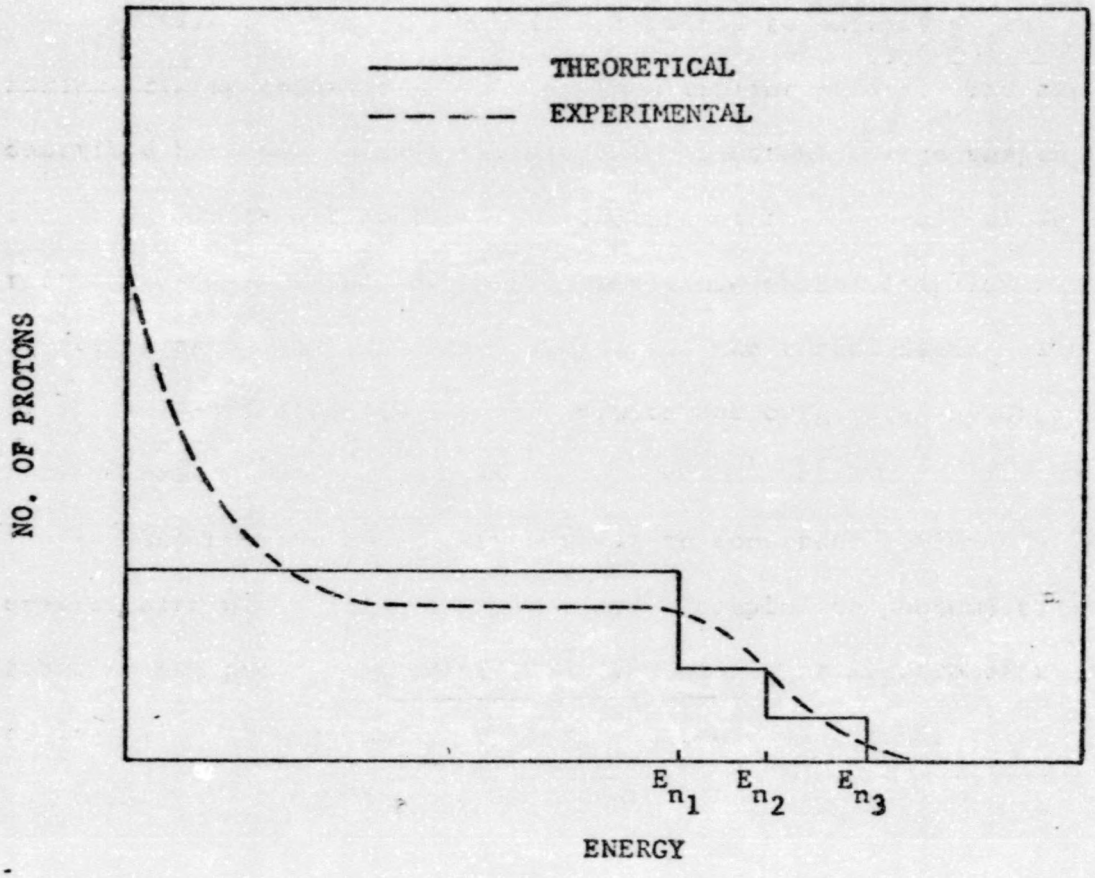

FIGURE 2 THE NUMBER OF RECOIL PROTONS AS A FUNCTION OF PROTON ENERGY WITH THREE ENERGY GROUPS CLOSELY SPACED.[2]

from which the energy can be computed. The time-of-flight spectrometer can also be used with a wider range of neutron energies since inelastic interactions in the detector no longer present a problem.

There are many electronic approaches to extracting the maximum timing information from photomultiplier pulses.[3,4,5] The circuit described here uses a snap-off diode for constant charge shaping in conjunction with a tunnel diode. The use of the snap-off diode reduces the walk caused by varying amplitude photomultiplier signals by acting as a constant charge shaper for the tunnel diode. The use of the snap-off diode in timing circuits was originated by Grunberg and Tepper.[6]

The purpose of this thesis was to construct a time-of-flight spectrometer using plastic scintillators coupled to photomultiplier tubes as the primary detectors. A time-of-flight spectrometer with at least 2.0 nanoseconds of time resolution was desired.

II. THEORY AND CONSTRUCTION FEATURES

The Theory of a Time-of-Flight Spectrometer

A time-of-flight spectrometer is based on the precise timing of the interval between two events. If two particles are emitted in coincidence from a radioactive source, one particle can be detected with one detector and the other particle with another detector. The time interval between these two detection events can be determined. This time interval can be related to the flight path of the two particles to find their time-of-flight from source to detector.

The main requirements placed on the timing circuits are that they be fast (nanosecond timing), that they be able to handle a wide range of input signal magnitudes, and that they be able to handle high count rates without appreciable loss of time resolution.

Each channel of the time-of-flight spectrometer consists of a Nuclear Enterprise NE-102 plastic scintillator optically coupled to a photomultiplier tube, a voltage divider for proper photomultiplier dynode bias, a current limiter, a constant charge shaper, and a timing pulse output circuit. One timing pulse output is used as the start signal and the other for a stop signal for controlling the time-to-amplitude converter. The output of the time-to-amplitude converter is coupled to a multichannel pulse height analyzer.[7]

The Photomultiplier Tube

The photomultiplier tube is made up of a photosensitive cathode followed by a series of secondary emitters called dynodes, which are maintained at appropriate potentials. Light which falls on the photocathode releases electrons and these electrons are accelerated to the first dynode. The dynodes are made of a material which is a good secondary emitter of electrons. Thus, more electrons are emitted from each dynode than are incident upon it. A suitable arrangement of dynodes causes these electrons to be attracted to the next successive dynode, and so on. Typical values of gain for a 14-stage multiplier are 10^8 for an applied overall voltage of 2.2 kV. The overall gain varies rapidly with the applied voltage which should in general be kept constant to 0.1 per cent.[8]

The photocathode spectral sensitivity is a variable depending on the material used. It is necessary that the spectral emission of the scintillator approximately match the spectral sensitivity of the photocathode. Sometimes wavelength shifters are used in order to more closely match the photocathode.[8]

The Snap-Off Diode

The snap-off diode is a very important part of the timing circuit. The function of the snap-off diode is to transform the variable amplitude input signal to a constant charge.

When the ordinary diode is biased in the forward direction, there is a stored charge in the diode given by the equation[9]

$$Q_s = I_f \tau (1 - e^{-t/\tau}) \qquad 2\text{-}1$$

where Qs is the stored charge, I_f is the forward current amplitude, τ is the life time of the minority carrier, and t is the time. For long conduction times we have

$$Qs \approx I_f \tau . \qquad 2\text{-}2$$

The charge distribution as a function of distance from the junction in an ordinary diode is exponential (Fig. 3a).[6] When a reverse current step is applied to the diode, reverse conduction occurs until the stored charge is removed from the diode. There are roughly two stages following the application of the reverse current step. The carriers in the immediate vicinity of the junction are removed during the first stage while the resistance is very low. In the second stage the resistance (determined by diffusion and recombination) increases to higher and higher values. In the ordinary diode the charge removed during the first stage is small compared to the total charge, and the boundary between the two stages is not too clearly defined.[6]

Unlike the ordinary diode the snap-off diode has a graded profile of the impurity concentration near the junction (Fig. 3b). This makes a junction characteristic which causes approximately 80 per cent of the stored charge to be discharged during the first stage and the transition between stages is very abrupt, lasting from 0.1 nanosecond to 0.2 nanosecond. It is possible to use the snap-off diode to produce short, constant charge pulses. If the snap-off diode is quiescently biased with a forward current, I_f, its stored charge is approximately given by equation 2-2.

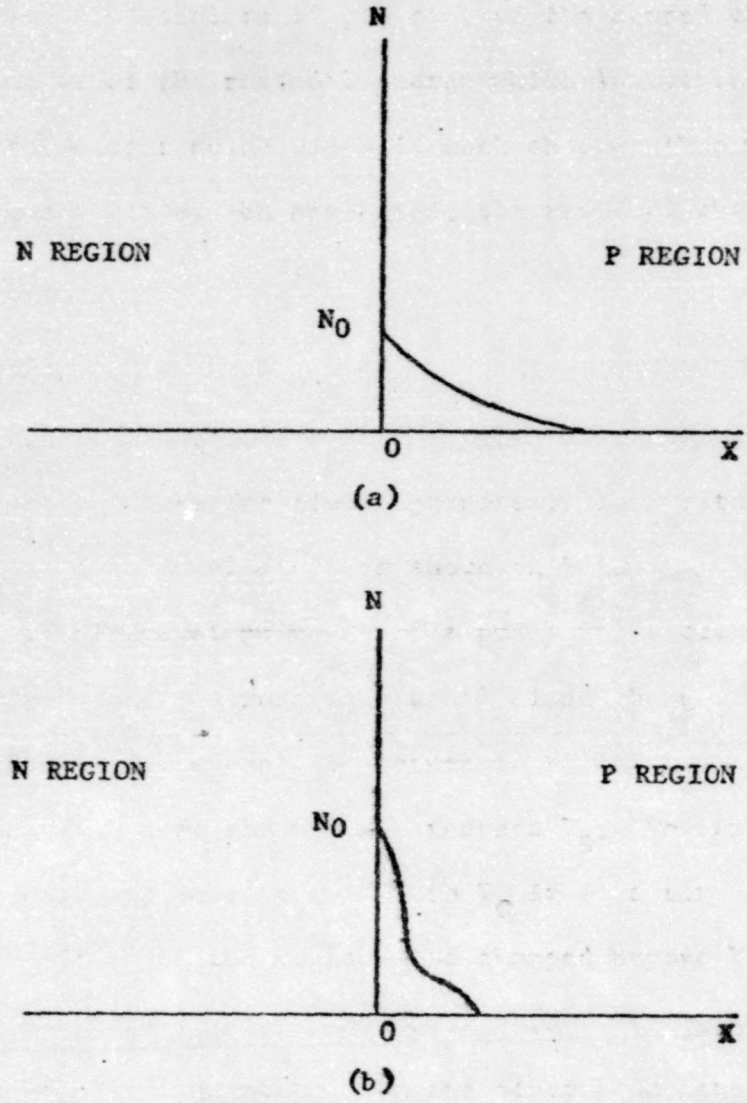

FIGURE 3 MINORITY CARRIER CHARGE DISTRIBUTION AS A FUNCTION OF DISTANCE FROM THE JUNCTION. a) ORDINARY DIODE; b) SNAP-OFF DIODE.[6]

$$Qs = I_f \gamma .$$

There is an output pulse consisting of two parts when a fast negative input pulse is applied. The first stage is the prompt pulse approximately equal to 80 per cent of the stored charge. The second is removal of the residual charge which leaves the diode more slowly. If the output pulse width is much shorter than γ, so that recombination effects can be neglected, the residual charge can be neglected.[9]

The Tunnel Diode

The tunnel diode is the device which allows the generation of a fast risetime pulse for timing purposes. The voltage-current characteristic of a tunnel diode is shown in Fig. 4.[9] If the tunnel diode is biased at point A and a pulse input current I_{in} is applied, the voltage across the tunnel diode changes beyond V_P toward V_C. The tunnel diode will return to V_A if at a time t_1, I_{in} is turned off before the voltage reaches V_B. Conversely, the tunnel diode will continue to switch to V_C if at a time t_2, I_{in} is turned off after the voltage has changed beyond V_B. The input charge given by $I_{in}\ t_1$ is not enough to switch the tunnel diode to the high voltage state. On the other hand, the input charge $I_{in}\ t_2$ is enough. The limiting case is when the charge is only sufficient to switch the tunnel diode to V_B. This is an unstable point and whether the tunnel diode returns to V_A or goes to V_C is determined by noise. Therefore, V_B is the pulse threshold

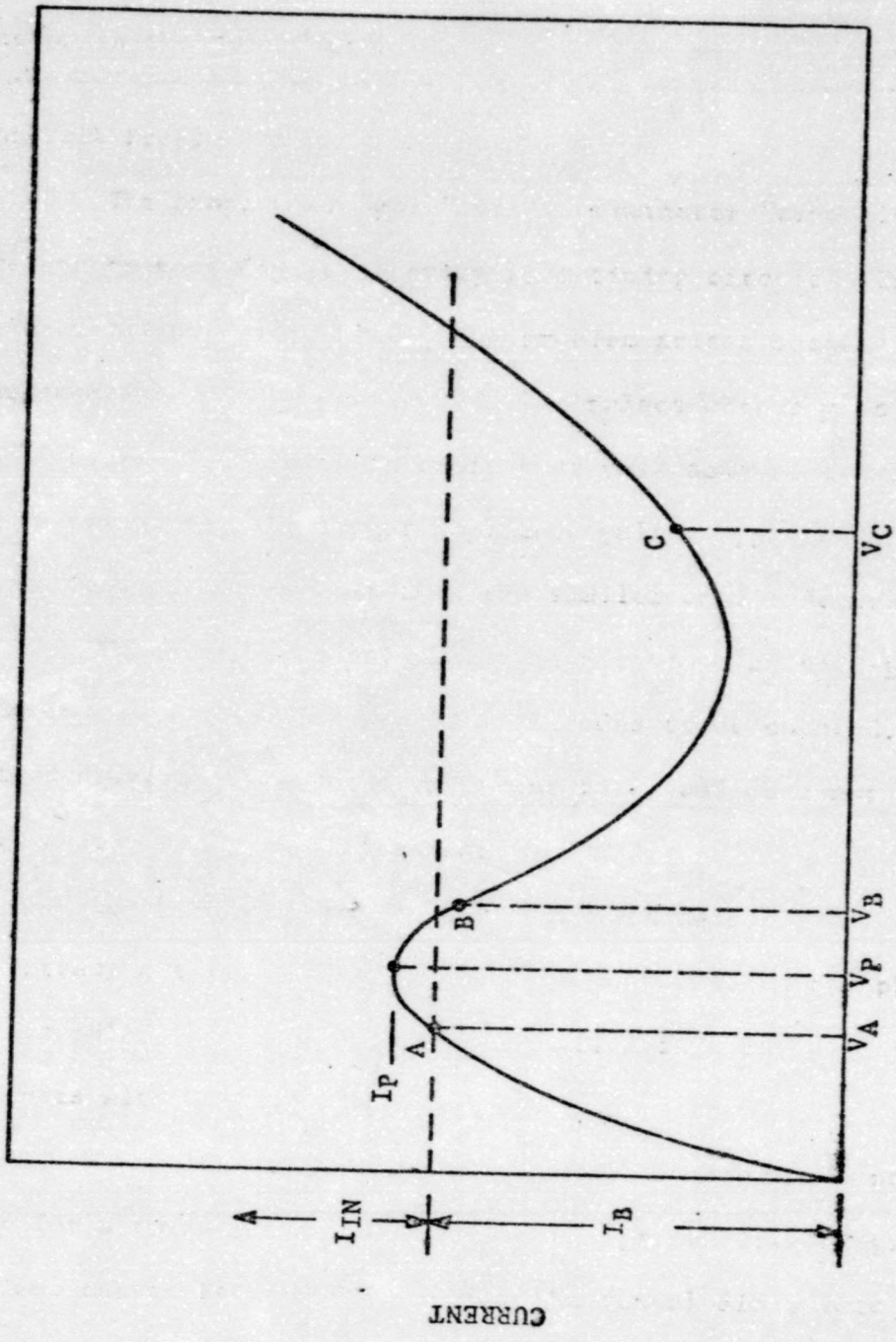

FIGURE 4 TUNNEL DIODE VOLTAGE AND CURRENT CHARACTERISTIC AND OPERATING POINTS(9)

voltage. The charge to arrive at V_B is the threshold charge for switching the tunnel diode into the high voltage state.[9]

The amount of charge used to switch the tunnel diode is a factor in the "walk" problem.

The Walk Problem

The problem of "walk" or discriminator "time slewing" is present to some degree in every fast timing circuit. In the neutron time-of-flight spectrometer, the problem arises because neutrons with the same energy give photomultiplier pulses with a wide range of amplitudes. Since every circuit must have some discrimination level to reject noise, the larger amplitude pulses appear to have reached the timing circuit sooner than the smaller amplitude pulses (Fig. 5).[6]

The time increment ΔT can be minimized by side-gating and allowing only a small range of magnitudes to be counted. Such a method drastically reduces the count rate, and does not improve the walk sufficiently in most cases.

The best that can be achieved with an electronic circuit is to extract all the timing information contained in the photomultiplier output pulse, and supply this information in a useful form to other circuits with no dead time.[3]

The much used picture of the walk in Fig. 5 is not exactly true for a tunnel diode used in the charge sensitive region. A minimum charge is needed to switch the tunnel diode into the high voltage state. Also, the magnitude of the charge overdrive determines the delay in the output pulse. A rough picture of the tunnel diode behavior is shown in Fig. 6.[9] The minimum charge

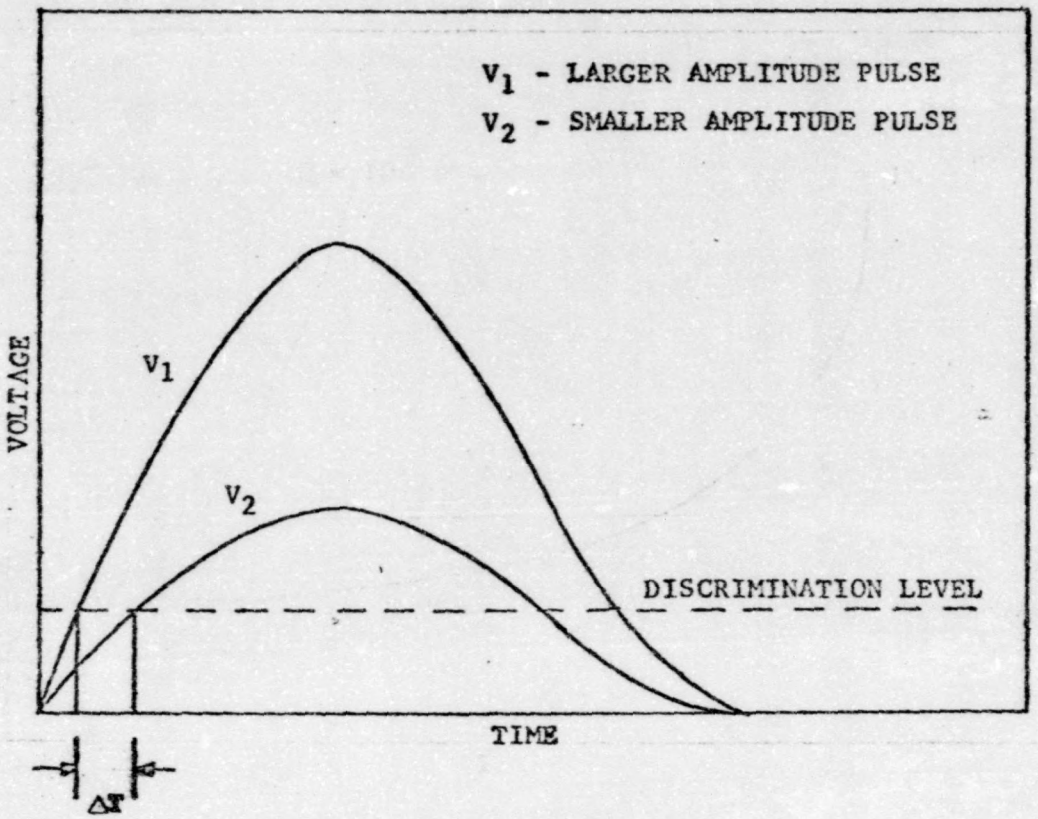

FIGURE 5 THE STANDARD WALK PICTURE.[6]

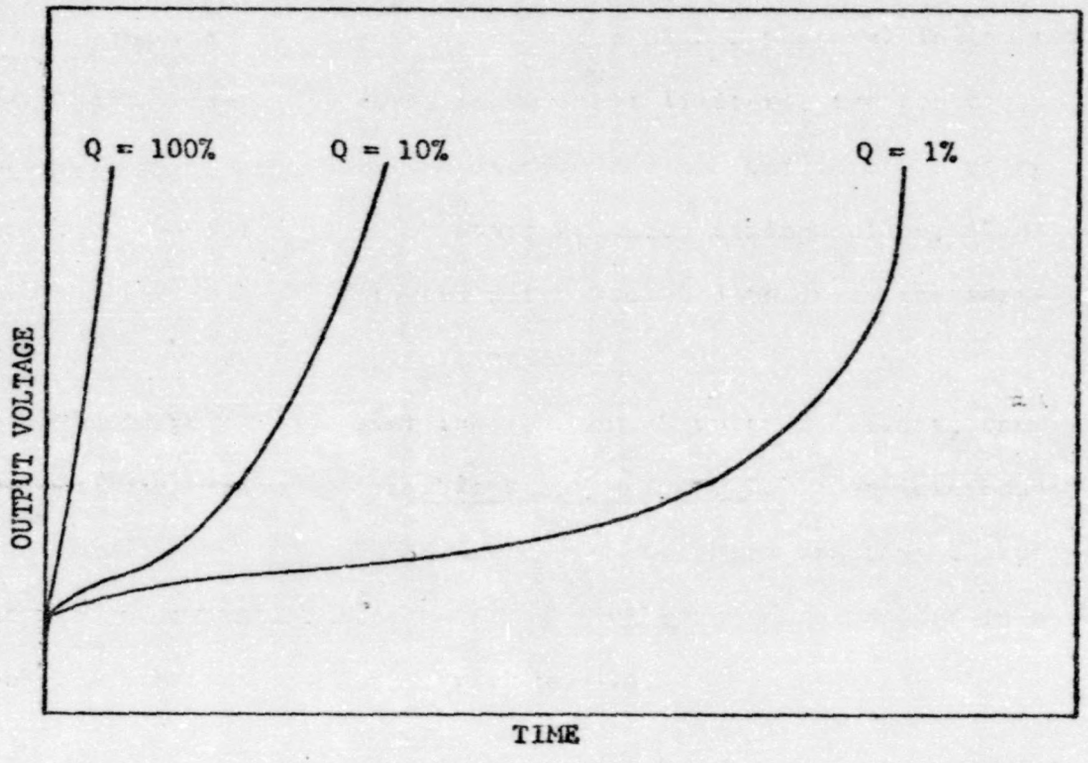

FIGURE 6 TUNNEL DIODE OUTPUT VOLTAGE RESPONSE AS A FUNCTION OF CHARGE OVERDRIVE Q.[9]

necessary to switch the tunnel diode into the high voltage state is supplied in each case, but the charge overdrive, Q, is different in each of the three cases. Therefore, the real walk with a tunnel diode is greater than the standard walk already mentioned unless the amount of charge overdrive is held constant. This is the purpose for using a snap-off diode to trigger the tunnel diode.

The Circuit Features

The circuits assembled were two 56 AVP photomultiplier tube bases with voltage dividers, two current limiters, two constant charge shapers using snap-off diodes, and two univibrators using tunnel diodes for generating start and stop timing pulses. Two double stage emitter followers were assembled to drive the fast-slow coincidence side-gating circuit.

One photomultiplier tube base with voltage divider, one current limiter, and one double stage emitter follower were mounted in each of two 3" X 4" X 5" chassis boxes. Both constant charge shapers and the start and the stop univibrator were mounted in a double width standard A.E.C. rack module.

The Photomultiplier Tube Base and Voltage Divider Circuit

The 56 AVP photomultiplier voltage divider is basically the one used by Tepper (Fig. 7).[10]

There are two voltage dividers suggested for the 56 AVP in the Amperex manual,[11] and one of these is intended for greater linearity than the other. The voltage divider used is one which is somewhere between the two given. This makes the anode pulse tend to saturate slightly with higher inputs to the photomultiplier tube.

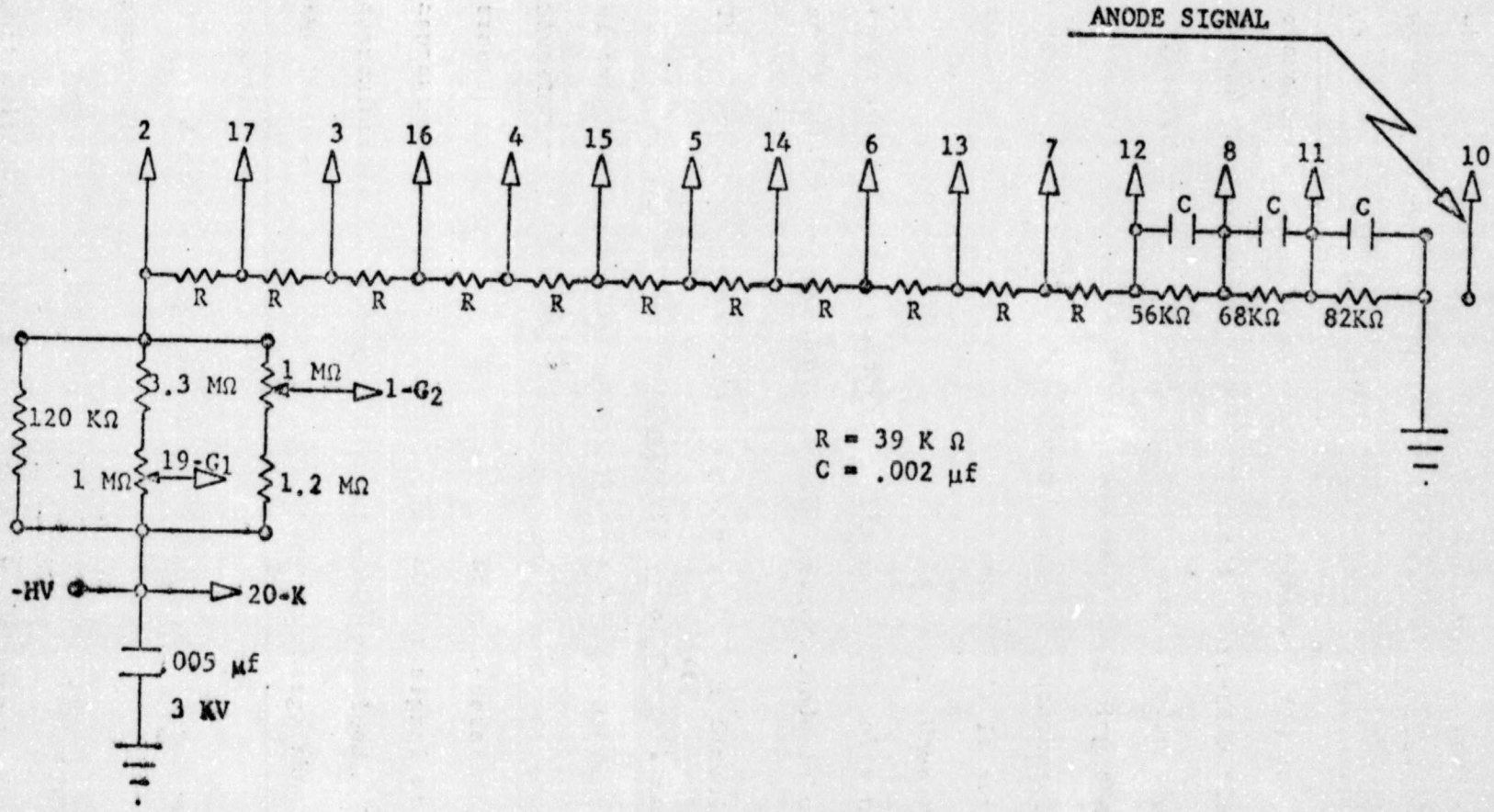

FIGURE 7 VOLTAGE DIVIDER FOR 56 AVP PHOTOMULTIPLIER TUBE.(10)

There are some features of the 56 AVP photomultiplier tube which should be discussed. The tube has 14 stages and has an anode pulse risetime of 2.0 nanoseconds. The potential of the focusing electrode g_1 to the photocathode can be adjusted to obtain several characteristics. These characteristics are (1) the collection of the largest anode signal, (2) the least transit-time fluctuations, (3) the collection giving the most constant output pulse amplitude, (4) the controlling of the useful cathode area by giving the electrode g_1 a negative potential with respect to the photocathode. When the potential of electrode g_1 to the photocathode is zero, approximately the center half of the photocathode is used. When the potential of electrode g_1 to the photocathode is made 100 volts negative, only a small portion in the center of the photocathode is used.[11]

The Current Limiter Circuit and Linear Output Circuit

The current limiter circuit (Fig. 8)[6] is located at the base of the photomultiplier tube. It is built on a print board and is a plug-in module for easy removal. The circuit uses diodes with a transistor to clip the input signal at a predetermined level of approximately 10 milliamperes. The output signal at this level is approximately 10 milliamperes into a 100 ohm load. The output of the limiter is connected to the constant charge shaper by a 92 ohm coaxial cable.

A double stage emitter follower is located on the same print board with the current limiter. The double stage emitter follower (Fig. 9) takes its input signal from the twelfth dynode of the photomultiplier tube, and it has a linear output. The circuit is

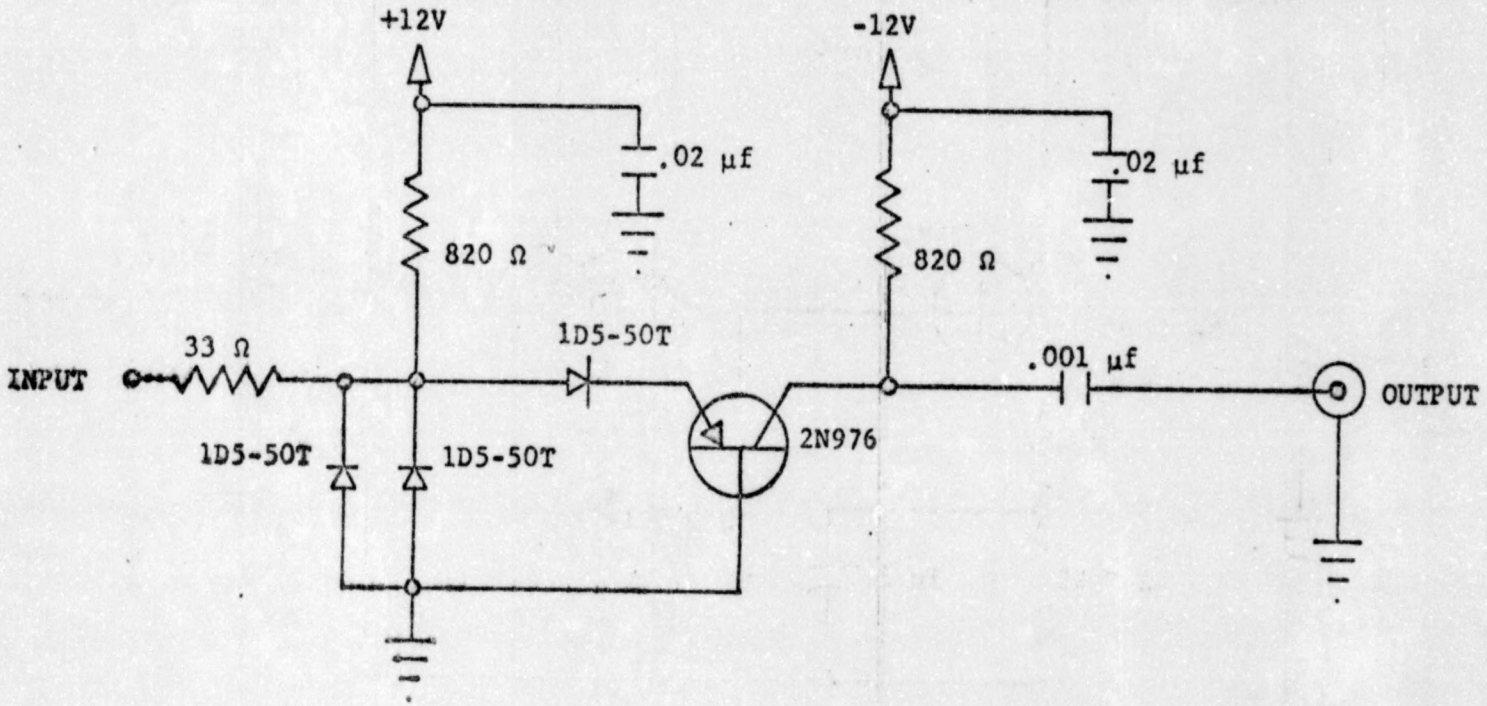

FIGURE 8 CURRENT LIMITER CIRCUIT.(6)

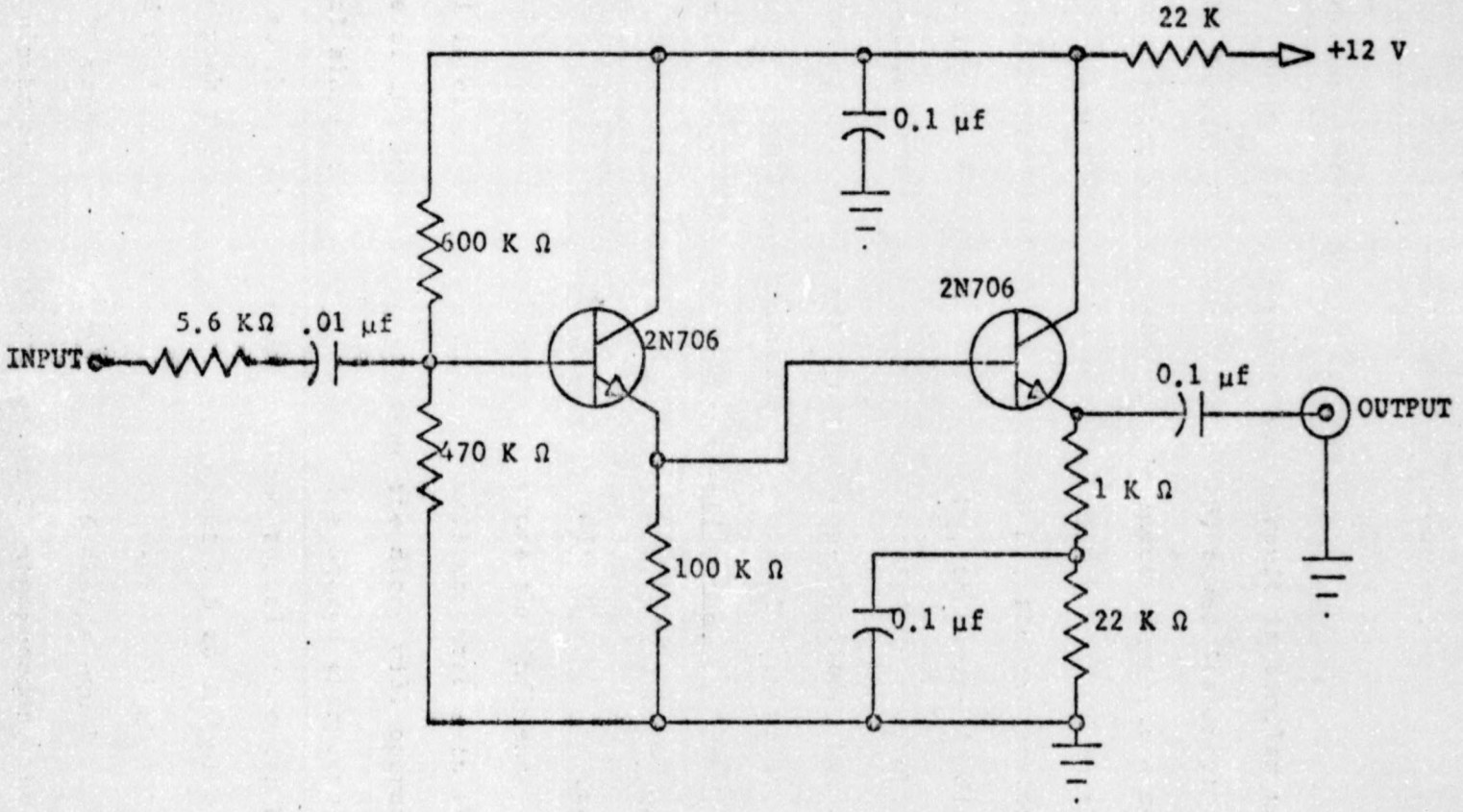

FIGURE 9 LINEAR OUTPUT CIRCUIT; DOUBLE STAGE EMITTER FOLLOWER.(12)

basically one used by Finlay,[12] and it is used to match the high impedance of the dynode with a 50 ohm cable. The linear output can be used with a single channel analyzer and coincidence circuit for side-gating the time-of-flight spectrometer.

The Constant Charge Shaper Circuit

The constant charge shaper circuit is similar to the one used by Tepper.[6] The circuit (Fig. 10) takes its input from the current limiter and transforms this input signal to a constant charge output. D_1 works as a low level discriminator. When the signal input is larger than the bias through D_1, the transistor, T_1, starts conducting and takes the charge off D_3, the snap-off diode. There are many small pulses from the photomultiplier tube which would continually change the bias on the snap-off diode, but a small bias current through D_1 eliminates nearly all of this noise. D_2 acts as a fast recovery diode for the snap-off diode.

The snap-off diode is chosen in the following way. The stored charge must be large compared with the charge transmitted through its capacitance, so as to reduce the influence of variable signal levels. It should also be small compared with the total charge of the input pulse, so that the diode will operate on the initial slope of the input pulse. The stored charge needs to be small so that the bias current of the tunnel diode can be set close to the peak for better accuracy. About 1.5 to 2.0 picocoulombs is a good choice. The snap-off diode hpa0154 has a guaranteed minimum τ of 20 nanoseconds. With the stored charge equal to 2.0 picocoulombs and τ of the order of 20 nanoseconds, the necessary

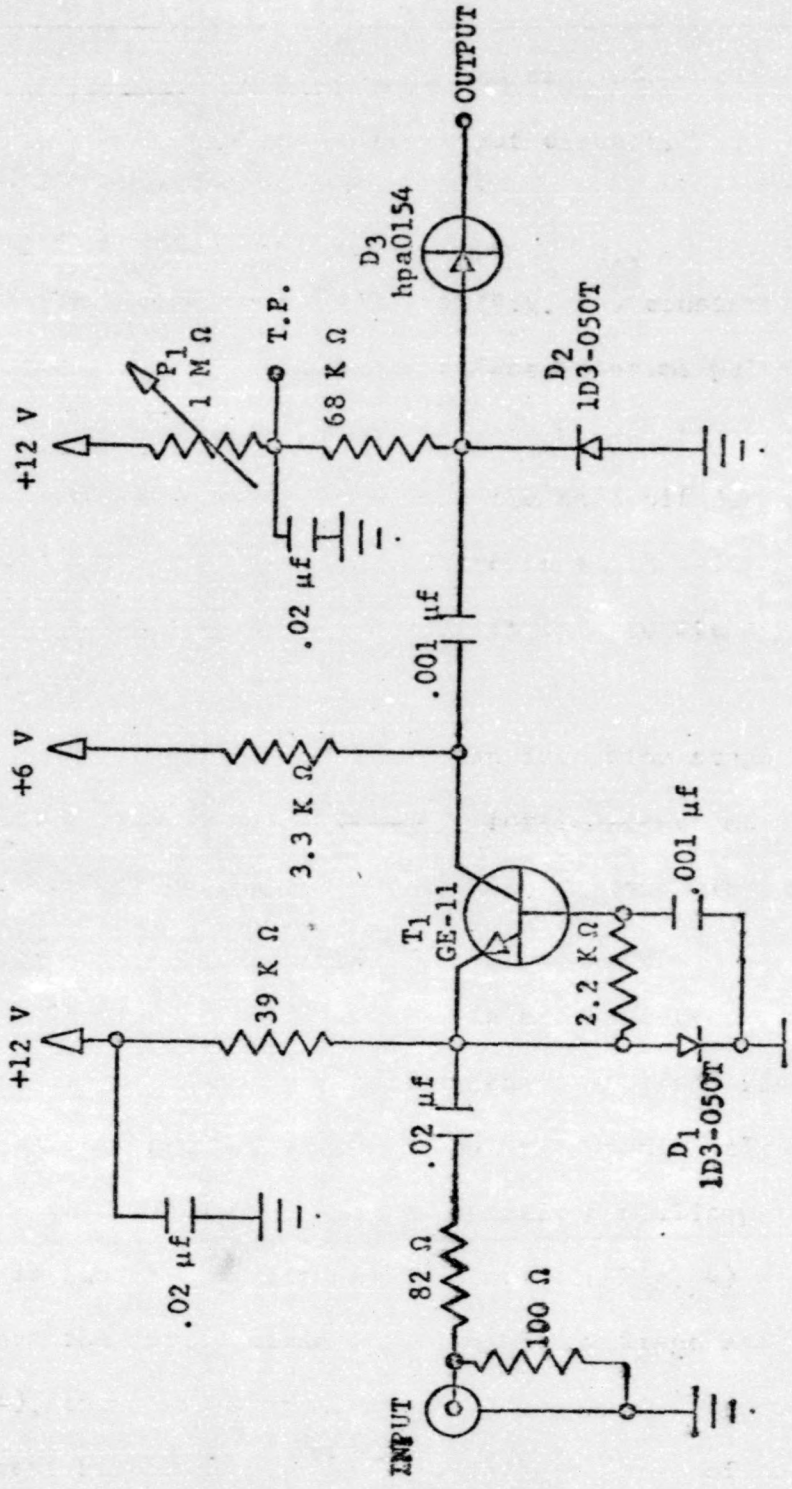

FIGURE 10 CONSTANT CHARGE SHAPER CIRCUIT.(6)

quiescent current from equation 2-2 is 100 microamperes. The potentiometer P_1 is used to adjust the quiescent bias current in the snap-off diode.

The charge removed from the snap-off diode is delivered into the tunnel diode in the pulse output circuit.

The Pulse Output Circuit

The pulse output circuit (Fig. 11)[6] consists of a transistor and a tunnel diode to generate a fast risetime pulse. The tunnel diode, TD254, is biased near its peak by adjusting P_2. When it receives the constant charge from the snap-off diode, it switches into its high voltage state. There is an immediate flood of base current in the transistor causing it to saturate and generate a very fast risetime pulse.

The second transistor is an inversion stage and the output transistor is an emitter follower for impedance matching the circuit to a 50 ohm cable. The output pulse magnitude is approximately one volt into a 50 ohm load.

The tunnel diode, TD254, is a high current diode. The high current is necessary in order to generate a fast risetime pulse. The peak current, Ip, of the TD254 is approximately 22 milliamperes and the valley current is approximately 6 milliamperes. When the TD254 is biased near its peak (Point A in Fig. 4) and a small charge switches the tunnel diode into its high voltage state (Point C in Fig. 4), there are approximately 12 to 14 milliamperes of the quiescent bias current that flow into the base of the 2N976

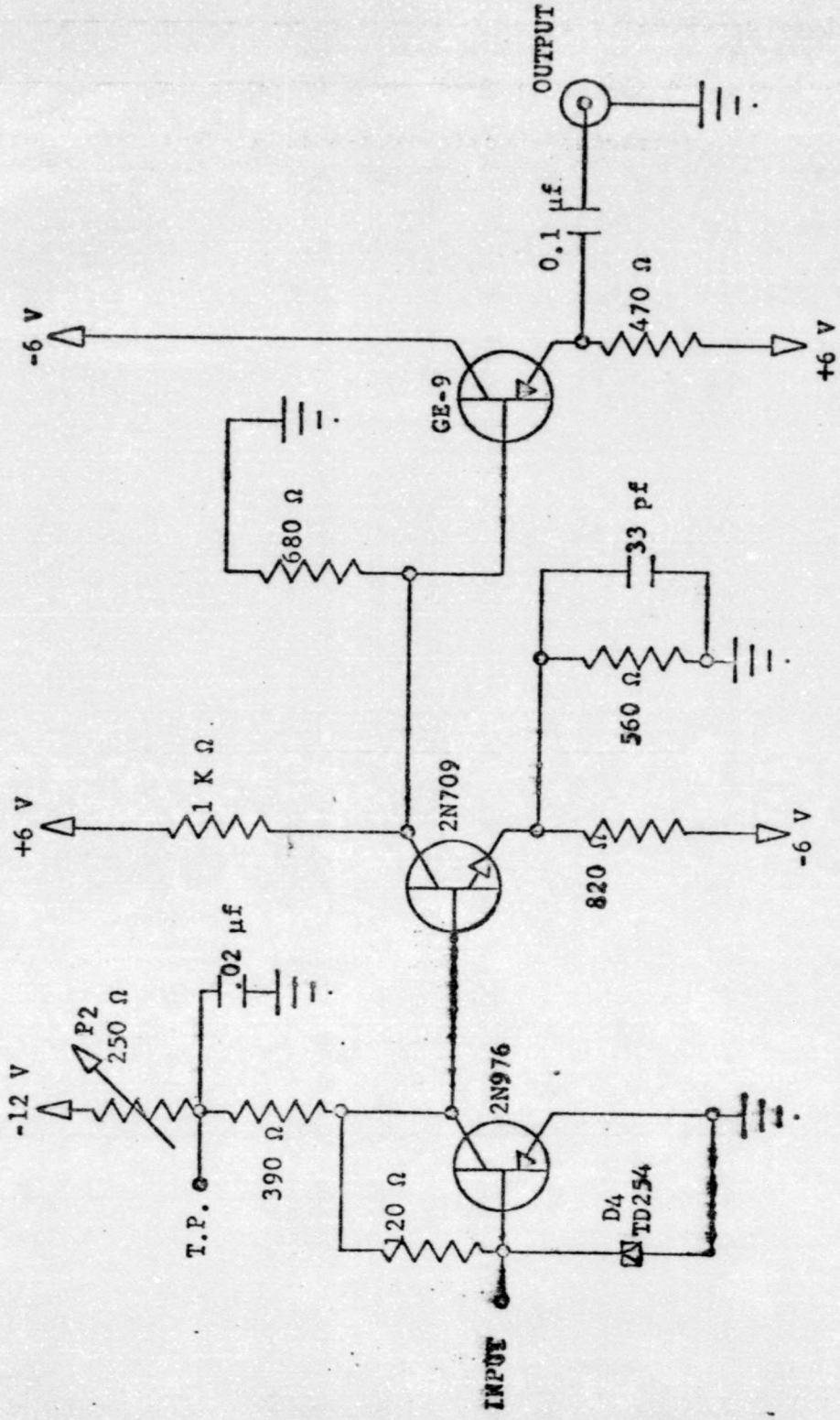

FIGURE 11 PULSE OUTPUT CIRCUIT.(6)

transistor. It is this flood of base current that causes the transistor to saturate and generate a fast risetime pulse.

The output pulse from one of these circuits is used as the start pulse and the output pulse from the other circuit is used as the stop pulse for the time-to-amplitude converter.

III. EXPERIMENTAL RESULTS

The Effects Using A Pulse Generator

Evaluation tests were conducted on each assembled circuit prior to operation as an integral unit. The tests were conducted using a Hewlett-Packard 214A pulser for a signal input and a Tektronix 585A real time oscilloscope with current and voltage probes for a signal monitor. This method of testing facilitates the location of faulty or improperly selected components. However, it suffers from the disadvantage of testing under idealized conditions and thus does not permit proper adjusting of all variables in the system.

The Linear Output Circuit

The emitter follower output circuit was tested using the pulser and oscilloscope. The pulser supplied a signal that normally would come from the twelfth dynode of the photomultiplier tube. The linear output was loaded with a 47 ohm resistor. The 47 ohm resistor was chosen because the circuit would be coupled with a 50 ohm coaxial cable to a circuit with a 50 ohm input impedance. The results of observations with the oscilloscope are presented in Table 1.

When the input is varied from 0 to 17.0 volts, the maximum deviation in the linearity of the output is 0.25 volts. At 20.0

TABLE 1

RESULTS OF TESTING THE LINEAR OUTPUT CIRCUIT WITH A PULSER AND OSCILLOSCOPE

INPUT (VOLTS)	OUTPUT (VOLTS)	
1.3	0.14	
1.6	0.20	
3.3	0.50	
6.5	1.10	
10.0	2.00	
13.5	2.80	
16.5	3.20	
20.0	3.60	(fall time increasing)
23.0	3.60	(fall time increasing)

Output was loaded with a 47 ohm resistor.

volts input, the output completely saturates. Since the input is taken from the twelfth dynode of the photomultiplier tube, the linearity within this range is sufficient for all cases in which the photomultiplier tube will be used.

The Current Limiter Circuit

The ability of the current limiter circuit to limit the anode signal was tested using the pulser and oscilloscope. The photomultiplier tube was not in the circuit during this phase of tests. The pulser was coupled through a capacitor to the input of the circuit and the output was loaded with 100 ohms. A 100 ohm load was chosen because the output will be coupled with a 92 ohm coaxial cable to a circuit with a 100 ohm input impedance. A current probe was used to measure the input current and a voltage probe was used to measure the output voltage. The results are presented in Table 2. From the data it can be observed that when the input current reaches 10 milliamperes the output begins to be limited, and as the input current is increased up to 400 milliamperes the output remains constant.

There was a noticeable amount of spurious oscillation at both the input and output when the input current was increased above 200 milliamperes. The source of the spurious oscillation was difficult to determine. Either the circuit or the network coupling the pulser to the circuit was causing the spurious oscillation. The ideal method for testing the circuit is under actual working conditions, that is with the photomultiplier tube in the circuit. The use of the photomultiplier tube with the scintillator and radioactive source to

TABLE 2

RESULTS OF TESTING THE LIMITER
CIRCUIT WITH A PULSER
AND OSCILLOSCOPE

INPUT (MILLIAMPERES)	OUTPUT (VOLTS)
5	0.5
10	1.0
50	1.0
100	1.0
150	1.0
200	1.0
250	1.0
300	1.0
350	1.0
400	1.0

Output was loaded with a 100 ohm resistor.

generate the test pulses was difficult because a repetitive pulse signal of constant magnitude was necessary in order to effectively observe all the characteristics of the signal. One method was to use a repetitive pulse light source in conjunction with the photomultiplier tube to generate the test pulses. A diode which emits a light pulse each time it is electrically pulsed was coupled to the photomultiplier tube and used to generate test pulses with the photomultiplier tube in the circuit. When a repetitive constant magnitude test signal such as this was used with the photomultiplier tube in the circuit, there was very little spurious oscillation at the anode of the photomultiplier tube or at the output of the current limiter circuit.

The Constant Charge Shaper and Pulse Output Circuit

Since the constant charge shaper circuit and the pulse output circuit when assembled were directly coupled together, it was necessary to test them as an integral unit. The bias setting for both the tunnel diode and the snap-off diode directly affects the operation of these circuits. There are several characteristics of operation that can be achieved by appropriately adjusting the bias on both the snap-off diode and the tunnel diode. According to Tepper,[6] the best time resolution should be achieved when the snap-off diode bias is as low as possible and the tunnel diode bias is as high as possible. However, when the circuit was set in this most sensitive mode of operation, it was unstable and vulnerable to spurious oscillation and noise from the other circuits. As the tunnel diode bias was lowered and the snap-off diode bias was raised, the circuit operated in a more stable manner. The bias settings at

this time were selected such that the input current could be varied over as wide a range as possible and still maintain stable operation.

With the above bias settings, the following tests were made. The pulser was coupled to the input and the output pulse was monitored with a sampling oscilloscope which behaves as a 50 ohm load. The presence of an output pulse and the output pulse shape were noted for different input voltages. The minimum input pulse necessary to obtain an output pulse was 0.85 volts, and the output pulse magnitude was 1.0 volt into a 50 ohm load. The risetime of the output pulse was approximately 2.0 nanoseconds, and the output pulse width was approximately 20 nanoseconds. An increase in the magnitude to 1.5 volts at the input resulted in no change in the output pulse shape or magnitude.

There was an unfavorable reflection of the input pulse to the constant charge shaper because of an impedance mismatch. A 100 ohm resistor was used to terminate the input of the circuit. This additional load on the limiting circuit necessitated an increase in the limiter current output.

The output of the current limiter circuit was then coupled to the input of the constant charge shaper circuit with a 92 ohm coaxial cable. The pulser was coupled to the input of the current limiter circuit and the output of the constant charge shaper circuit was loaded with 50 ohms. The output pulse had a constant shape and magnitude when the input current was changed from 10 milliamperes to greater than 400 milliamperes.

The Results Using Gamma Rays

After evaluation of the pulser test data and minor changes in components, the circuits were assembled as an integral unit to test the spectrometer under actual operating conditions. This test was conducted to establish the time resolution of the spectrometer using coincident gamma rays as timing signals.

The Experimental Setup

The experimental setup which was used in the time resolution evaluation is shown in Fig. 12. In both the start and stop detector, the anode signal is current limited before it reaches the respective constant charge shapers. In both the start and stop side, the charge from the snap-off diode is used to trigger the respective tunnel diode timing pulse generators. The start timing pulse is used to begin the time-to-amplitude conversion and the stop timing signal, after an appropriate delay, is used to stop the conversion process. The output from the time-to-amplitude converter is coupled to a multichannel pulse height analyzer.

A linear signal, the amplitude of which was proportional to the energy loss of the radiation in the scintillator, was taken from the twelfth dynode of the photomultiplier tube. An emitter follower was used to match the input impedance of a linear amplifier. The two linear amplifiers, two single channel analyzers and a fast coincidence module, constituted a standard fast-slow coincidence system. The base line and window width settings on the single channel analyzer permitted the selection of only predetermined pulse amplitudes from the photomultiplier tube, which were in coincidence, to be used for

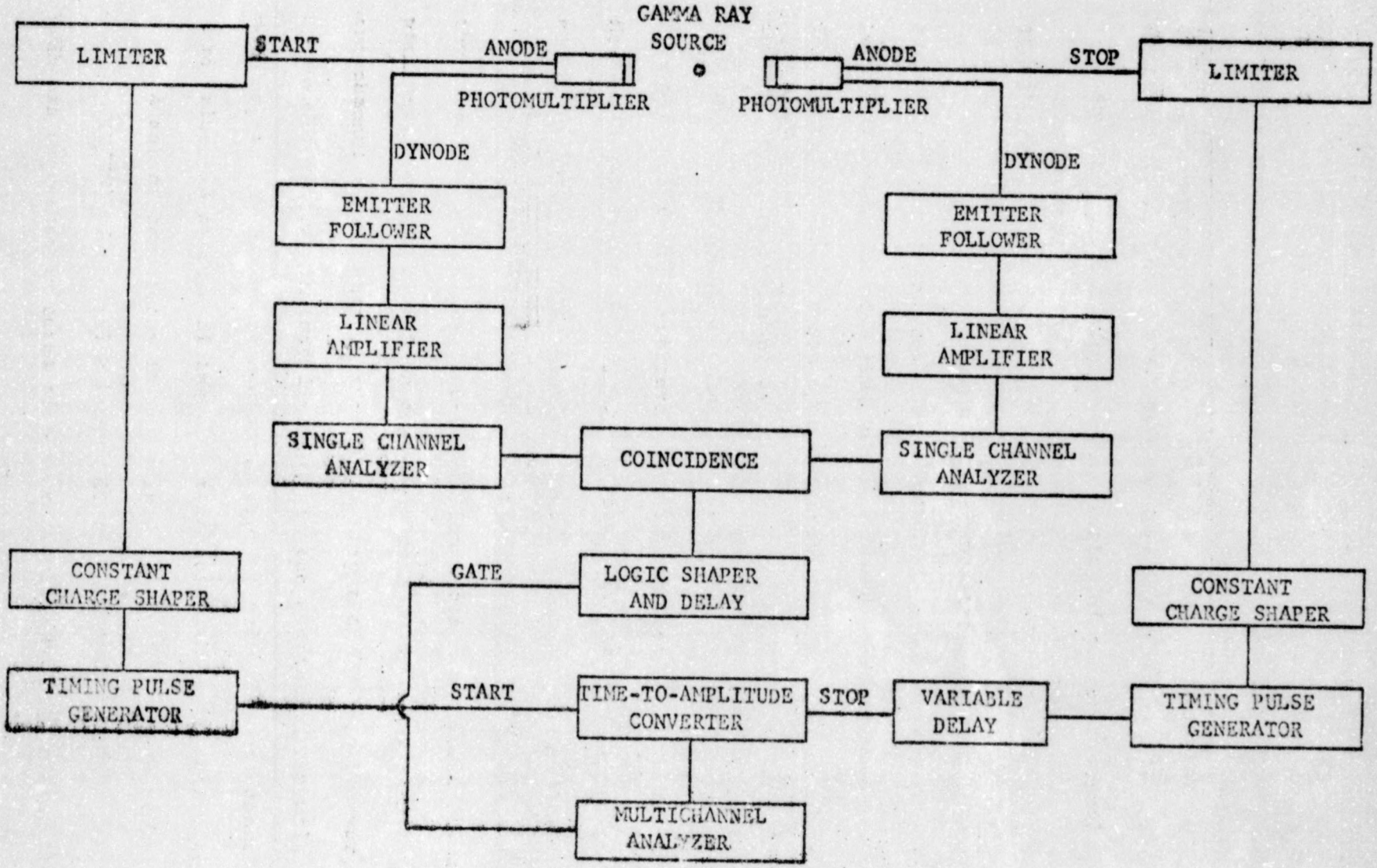

FIGURE 12 EXPERIMENTAL SETUP FOR GAMMA RAY TIME RESOLUTION

gating the multichannel pulse height analyzer input from the time-to-amplitude converter. This selection, often referred to as side-gating, was accomplished by using the output of the fast-slow coincidence system to open the linear gate at the input of the multichannel analyzer. The logic shaper and delay module was used to insure the correct time characteristics of the gate signal.

The Time Resolution Using Na^{22}

A Na^{22} source, which decays by positron emission, was used as a source of coincident gamma rays. The positron annihilation produces two 0.511 Mev gamma rays that are in coincidence. The ungated Compton scattered electron spectrum from one linear output is shown in Fig. 13. The different window width and base line settings are also shown with the appropriate energy scale. The maximum kinetic energy that a Compton scattered electron can receive from a 0.511 Mev gamma ray is 0.341 Mev. The energy scale in Fig. 13 is the energy of Compton scattered electrons.

If there were no timing uncertainties in the spectrometer, the output pulses of the time-to-amplitude converter would all be precisely the same magnitude and would appear as counts stored in one channel of the multichannel pulse height analyzer. However, because of several factors discussed in the section on the walk problem, there will be some distribution of pulse heights about the mean value. A measure of the time resolution of the spectrometer under a set of conditions is determined by the full width at half maximum (FWHM) of the pulse height distribution (Fig. 14). The FWHM was expressed in terms of time resolution by calibrating the

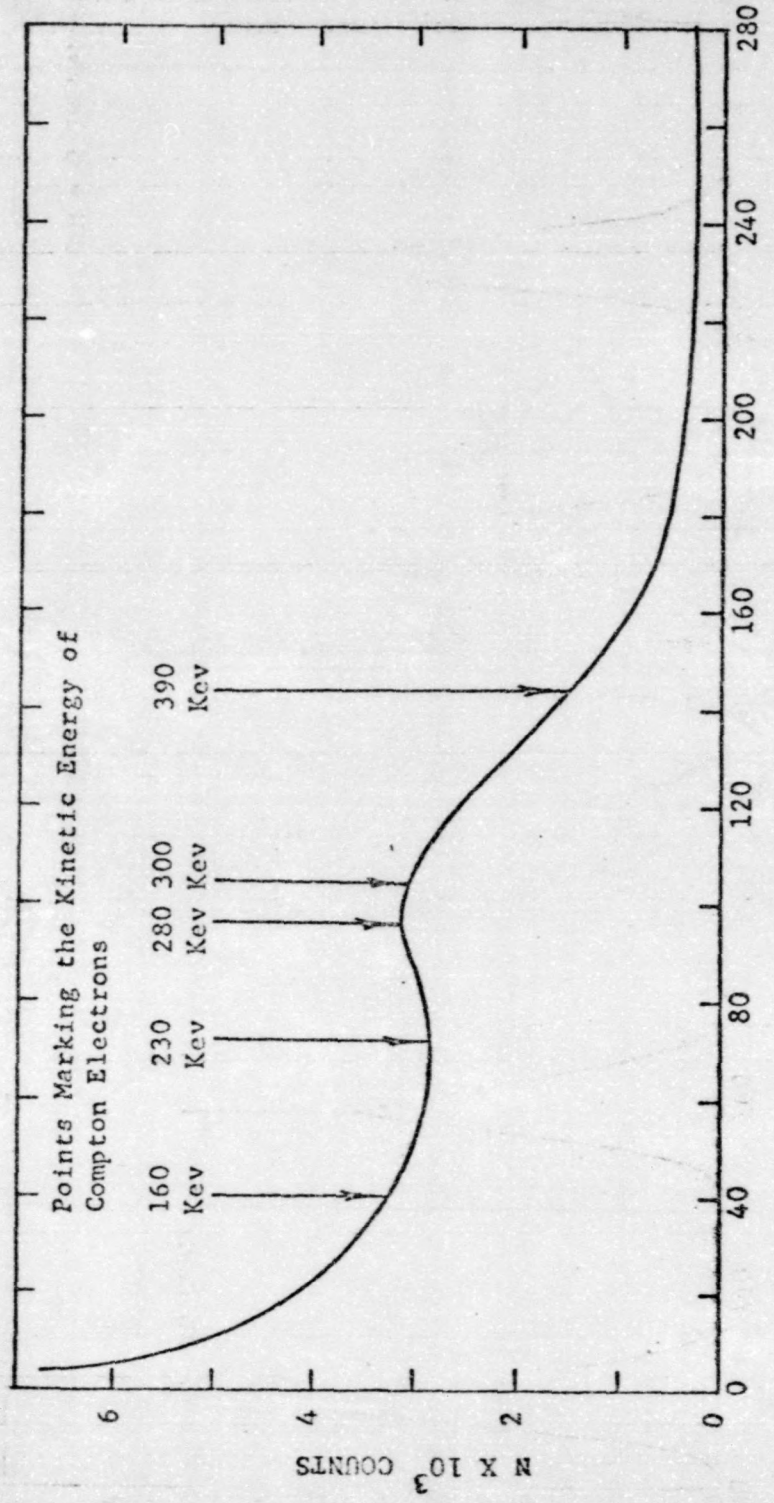

FIGURE 13 UNGATED NA^{22} SPECTRUM WITH ENERGY CALIBRATIONS FOR THE DIFFERENT WINDOW SETTINGS.

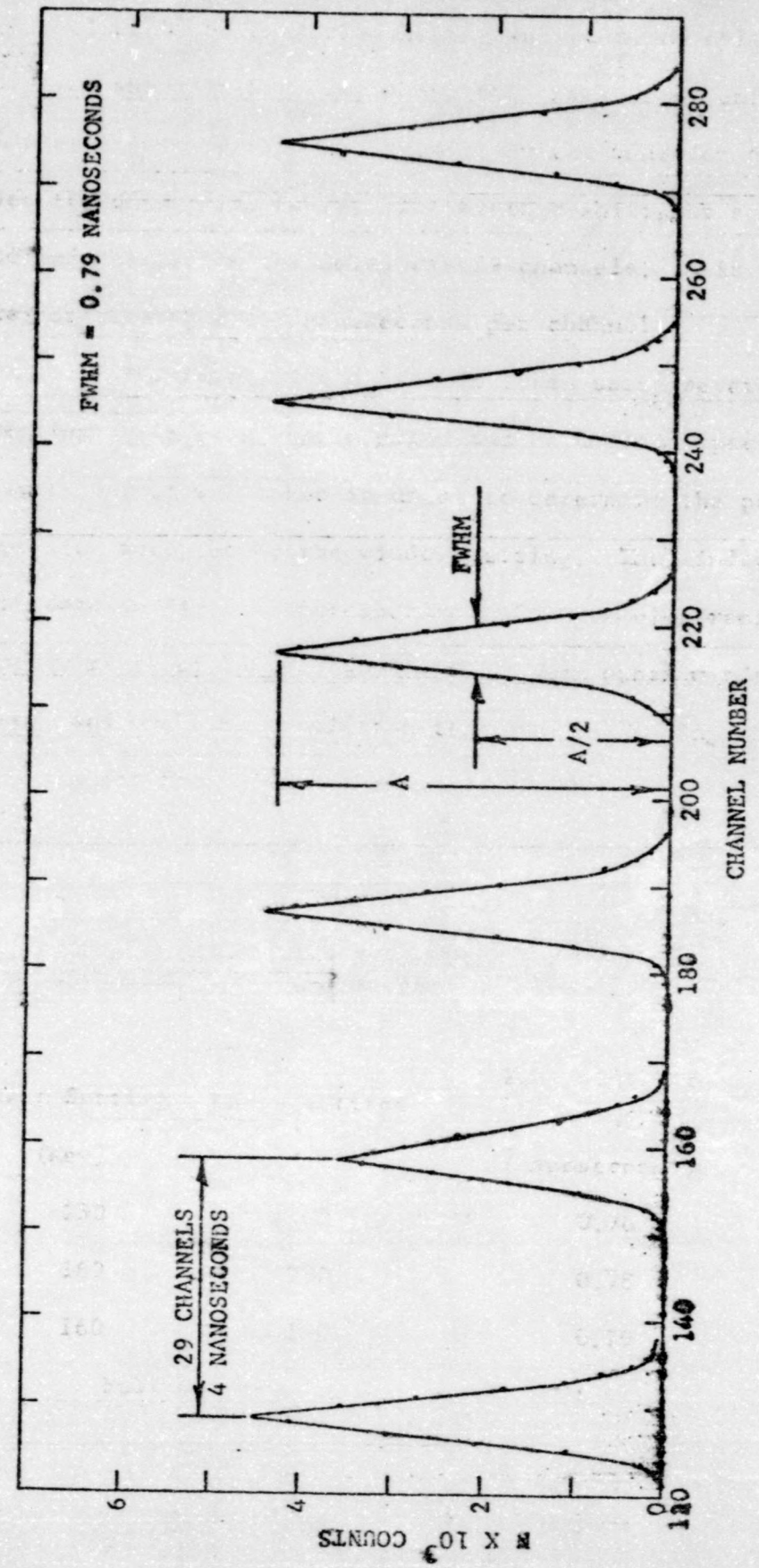

FIGURE 14 RESOLUTION DATA FOR NA^{22} FOR ONE WINDOW SETTING.

channel scale on the pulse height analyzer. A calibration display is also shown in Fig. 14, where each peak represents a change of 4 nanoseconds in the stop channel by the addition of calibrated lengths of coaxial cable. The average shift for several 4 nanosecond changes in the delay was 29 channels. This yielded a calibration of 0.138 nanoseconds per channel.

Time resolution data were taken using several window settings. In each case a gated and an ungated spectrum from one linear output was taken in order to determine the portion of the spectrum accepted by the window setting. The window setting for the data in Fig. 14 corresponds to Compton electrons with a kinetic energy range of 160 Kev to 390 Kev. Two other window settings were used, and one time resolution test was made using the full spectrum. The results from all four are shown in Table 3.

TABLE 3

THE TIME RESOLUTION USING Na^{22}
WITH FOUR WINDOW
SETTINGS

Lower Setting (Kev)	Upper Setting (Kev)	Full Width At Half Maximum (nanoseconds)	Full Width At 10 Percent Maximum (nanoseconds)
230	300	0.76	1.45
160	280	0.78	1.50
160	390	0.79	1.55
Full Spectrum		1.41	3.38

The window setting is varied over a wide range, but the time resolution is essentially the same in each case where side-gating was used. The full width at 10 per cent maximum is less when the smaller energy window is used. This narrow base width would be valuable if a low intensity energy group were located near a high intensity energy group.

The spectrometer was evaluated using a high count rate in the stop detector. The normal gated count rate in both the stop and the start detectors was approximately 1500 counts per minute. Extra sources were added to the stop detector so that the count rate in the gated stop detector was approximately 12,000 counts per minute. The FWHM using the window setting and the normal count rate in the stop detector was 0.76 nanoseconds. The FWHM using the same window and the high count rate in the stop detector was 0.83 nanoseconds. The FWHM using no gating and the high count rate in the stop detector was 1.59 nanoseconds. The window setting was such that Compton electrons with an energy range of 230 Kev to 300 Kev were accepted.

The spectrometer was evaluated by changing the window setting in steps over the Compton scattered spectrum. First, the baseline was such that Compton electrons down to zero energy were always accepted while the window width was varied over several settings to accept Compton electrons with a maximum energy of 550 Kev. Second, the baseline and window width were varied such that the upper Compton electron energy accepted was always 540 Kev while the lower Compton electron energy was varied over several settings. The results are shown in Table 4.

TABLE 4

THE TIME RESOLUTION USING Na^{22}
WITH WINDOW SETTINGS VARIED
OVER THE COMPTON SPECTRUM

Lower Setting (Kev)	Upper Setting (Kev)	Full Width At Half Maximum (nanoseconds)
0	550	1.11
0	410	1.59
0	260	1.66
0	120	1.73
110	540	0.97
250	540	0.69
395	540	0.62

It can be observed that the best time resolution (FWHM = 0.62 nanoseconds) was achieved with a small energy window at the high energy portion of the Compton spectrum. The time resolution was poorest when a small energy window at the low energy portion of the Compton spectrum was used.

The Time Resolution Using Co^{60}

The spectrometer was evaluated using Co^{60} as a source of higher energy gamma rays. The Co^{60} source emits a gamma ray with 1.17 Mev energy immediately followed by another gamma ray with 1.33 Mev energy. The maximum kinetic energy of the Compton electrons associated with these two gamma rays is 0.96 Mev and 1.12 Mev

respectively. Time resolution data were taken using two window settings. The results are shown in Table 5.

TABLE 5

THE TIME RESOLUTION USING Co^{60} WITH TWO WINDOW SETTINGS

Lower Setting (Kev)	Upper Setting (Kev)	Full Width At Half Maximum (nanoseconds)	Full Width At 10 Percent Maximum (nanoseconds)
660	890	0.90	1.66
660	780	0.79	1.31

The Co^{60} time resolution using the smaller window setting is approximately the same as with the Na^{22} source.

IV. SUMMARY AND CONCLUSIONS

Accomplishment of Purpose and Objectives

The primary objective of achieving at least 2.0 nanoseconds of time resolution (FWHM) using a wide range of pulse heights was realized under all test conditions. The best time resolution obtained was a FWHM of 0.62 nanoseconds, using a narrow range of pulse heights. However, the FWHM increased to only 1.41 nanoseconds when the full range of pulse heights from the photomultiplier tube was used. The full width at 10 per cent maximum was 1.45 nanoseconds when using narrow side-gating. This increased to 3.38 nanoseconds when using no side-gating. The FWHM increased from 0.76 nanoseconds to 0.83 nanoseconds when the count rate in the stop detector was increased by eight fold.

The spectrometer was checked using different tunnel diode and snap-off diode bias points. According to Tepper,[6] as discussed in the section on the constant charge shaper and pulse output circuit, the time resolution should be better when the snap-off diode bias is as low as possible and the tunnel diode bias is as high as possible. The time resolution using gamma rays was better when the snap-off diode bias was higher than suggested earlier. The tunnel diode walk, as previously discussed (Fig. 6), is affected by a variable charge input. When the snap-off diode was biased at a higher level, there was more stored charge in the diode, and there

was sufficient charge overdrive from the smaller input pulses to guarantee faster switching of the tunnel diode. The results from Table 4 support this conclusion. The time resolution was poorest when the window setting was such that only small input pulses were accepted.

Areas for Further Effort

The time-of-flight spectrometer in its present state has two direct applications in experiments. The first application is in the area of fast neutron scattering. In this case, the start conversion is begun by the detection of an associated particle which is produced in an accelerator along with the neutrons. The stop conversion pulse is initiated by the detection of the neutrons scattered from a target. The second application is in the determination of the lifetime of the excited states of nuclei. The life of the excited states within nuclei range from several hours to 10^{-16} seconds. The determination of the lifetime of an excited state yields useful information about the spin and parity of the level of the state. The upper limit of this spectrometer for this application is about 10^{-11} seconds.

Recently a new technique for extracting the maximum timing information from photomultiplier tube pulses has been developed. (13) This allows a FWHM of 0.5 nanoseconds over a 100 to 1 dynamic range. A spectrometer with better time resolution and a greater dynamic range could be constructed using this better technique.

LIST OF REFERENCES

1. Swartz, C. D., and Owen, G. E., "Recoil Detection in Scintillators," in Fast Neutron Physics, ed. by J. B. Marion and J. L. Fowler, Interscience Publishers, Inc., New York, 1960, p. 220.

2. Swartz, C. D., Owen, G. E., and Ames, O., A.E.C. Contract AT(30-1) - 2028 (1957).

3. Bjerke, A. E., Kerns, Q. A., and Nunmaker, T. A., "Pulse Shaping and Standardizing of Photomultiplier Signals For Optimum Timing Information Using Tunnel Diodes," Nuclear Instruments and Methods 15, 249-267 (1962).

4. Gibbons, F. L., "A Nanosecond Neutron Time-Of-Flight Spectrometer Using Avalanche Transistors," IEEE Transactions on Nuclear Science 13, 305-310 (1966).

5. Wieber, D. L., and Lefevre, H. W., "An Amplitude - Independent Nanosecond Timing Discriminator for Fast Photomultipliers," IEEE Transactions on Nuclear Science 13, 406-412 (1966).

6. Grunberg, J. and Tepper, L., "Fast Timing Circuits Using Storage Diodes," IEEE Transactions on Nuclear Science 13, 389-393 (1966).

7. Nuclear Enterprises, Ltd., Scintillator Catalogue, Winnipeg 21, Manitoba, Canada.

8. Allen, W. D., Neutron Detection, Philosopical Library, Inc., New York, 1960, pp. 73-76.

9. Sear, B. E., "Charge Controlled Nanosecond Logic Circuitry," Proceedings of the IEEE 51, 1215-1227 (1963).

10. Tepper, L., Private Communication.

11. Amperex Electronic Corporation, Photomultiplier Tubes, Nuclear Associates, Inc., New York, 1965, Tube Type 56 AVP, p. 4.

12. Finlay, R. W., "Scattering of Fast Neutrons in Light and Medium Nuclei," NSF Final Report G-P 1848, Ohio University, Athens, Ohio, December, 1965, p. 19.

13. Ortec, Inc., Oak Ridge, Tennessee.

BIOGRAPHICAL SKETCH

Mr. David K. Moorman was born on January 4, 1939, at Glen Dean, Kentucky. He was graduated from Breckinridge County High School in May 1957. Having enlisted in the U. S. Army Reserve in April 1956, he entered the U. S. Army for six months of active duty.

In September 1958, he entered Western Kentucky University as a full time student. A second tour of active duty in the U. S. Army from October 1961 to August 1962 interrupted his college career. Two years later he received an honorable discharge from the U. S. Army Reserve. He was awarded the Bachelor of Science Degree in Physics and Mathematics by Western Kentucky University in May 1963. While at Western Kentucky University, Mr. Moorman received the Beginning Physics Achievement Award; and he was a member of the Math Club, Physics Club, Student Council, and Sigma Pi Sigma Physics Honor Society. He also served as president of the Math Club and Sigma Pi Sigma.

Mr. Moorman joined the engineering staff of the Tube Department of the General Electric Company at Owensboro, Kentucky, in June 1963. His initial assignment as a design engineer was in the area of photoconductive materials used in photoconductive cells. Later, he became a product design engineer of planar triodes of ceramic and metal construction. Effort was directed primarily toward the design of microwave tube energy sources.

In September 1963, Mr. Moorman enrolled in the Western Kentucky University Graduate School to begin work on a Master of Science Degree in Engineering Physics.

Mr. Moorman is married to the former Doris Lyons, and they have two sons.